

Structural, Mechanical and Optical Properties of PVA Doped with TiO₂ and ZnO Nanoparticles

Gananatha Shetty B^{1a}, Vincent Crasta^{2b}, Rithin Kumar N B^{3c}, Rajesh K^{2d}

¹Department of Physics, Alva's College, Moodbidri -574227, Karnataka, India

²Department of physics, St. Joseph Engineering College, Vamanjoor, Mangaluru- 575028 Karnataka, India

³Department of physics, A.J Institute of Engineering and Technology, Mangaluru- 575006 Karnataka, India

^bCorresponding author E-mail: vincentc@sjec.ac.in

Email: ^agananathshetty@rediffmail.com, ^crithin4u@rediffmail.com, ^drajeshyethadka@gmail.com

Abstract: This article emphasizes the preparation of TiO₂, ZnO nanoparticles and PVA/(x)TiO₂(15-x)ZnO nanocomposites for x = 0%, 1%, 5%, 7.5%, 10%, 14% and 15% doping concentration via solution casting method. The micro structural studies of prepared nano films were studied using x-ray diffraction (XRD) technique. The UV – Visible spectra reveals the severe decrease in optical energy gap of nanocomposites for x=14% doping concentration. Universal testing machine (UTM) shows high tensile strength, stiffness and Young's modulus for x=14% doping concentration.

1. INTRODUCTION

In recent years, the nanoparticles have attracted wide scope in scientific field due to its unexpected outcomes in their molecular as well as atomic states [1]. Metal oxide nanoparticles proved to be one of the significant materials for device application due to its multifaceted properties [2, 3]. Zinc oxide nanoparticle (ZnO) is one of the cost effective nanoparticles having plethora of application in solar cells, photo catalysis, drugs and chemical sensors [4-6]. On the other hand, Titanium dioxide nanoparticles (TiO₂) also substantiates to be unsurpassed dopants owing to its plentiful benefits, such as economy, green environment, non-toxicity, high photo catalytic activity, optical and electronic properties, antibacterial activity and UV protection [7]. These nanoparticles when embedded on polyvinyl alcohol (PVA, MOWIOL10-98) matrix, they play a vital role in enhancing its properties [8]. The present paper deals with the preparation of PVA(x)TiO₂/(15-x)ZnO nanocomposites for x=0, 1, 5, 7.5, 10, 14 and 15wt% concentration via solvent casting method.

2. EXPERIMENTAL DETAILS

2.1 Preparation of Titanium Dioxide nanoparticles

The compounds used for the preparation of Titanium dioxide (TiO₂) nanoparticles were procured from Sigma Aldrich, Germany. Liquid A is prepared by mixing 8ml dibutyl phthalate with 20ml of absolute ethyl alcohol, kept in a temperature controlled magnetic stirrer with stirring rate 800rpm for an hour. Liquid B is prepared by dissolving 15g of ammonium sulphate in 60ml of de-ionized water and 6ml of Hydrochloric acid. Then liquid A is mixed with liquid B at temperature 850C and kept on magnetic stirrer at 600rpm until the solution becomes a complete turbid formation. Then ammonium is added drop wise till the turbid solution turns milky white. The solvent is allowed to deposit for 24 hours and clear solution is filtered. The residue at the bottom is washed recurrently with de-ionizing water till the pH of the solution turns neutral. Later the neutral residue is filtered using 0.1µm Whatman Nylon filter membrane. The obtained precursor is dried at 550°C muffle to bake for 2 hours to get titanium dioxide (TiO₂) nanoparticles.

2.2 Preparation of zinc oxide nanoparticles

The NaOH and Zn(NO₃)₂·6H₂O chemicals were procured from Sigma Aldrich, Germany. 40g of NaOH is dissolved in 1 litre of de-ionized water and heated up to 80°C kept in temperature controlled magnetic stirrer at

1000 rpm for one hour. For this 0.5M Zn (NO₃)₂·6H₂O was added and the mixture was further kept on magnetic stirrer with stirring rate of 1000rpm for two hours at 80°C. The precipitated solution formed from the above reaction was separated using a centrifuge to obtain ZnO. The residue is washed several times with de-ionized water until all the traces of NaOH are removed. The obtained ZnO nanoparticles were then dried at 90°C and kept in oven for about 8 hours.

2.3 PVA nanocomposites Sample preparation

8g PVA (Mowiol 10-98, Sigma Aldrich Germany) is mixed with 180ml of distilled water and heated up to 80°C kept under constant stirring at 1200rpm till a clear viscous PVA solvent is obtained. The PVA solvent is cooled to room temperature. To avoid the formation of aggregation stirring is continued using mechanical stirrer at 250rpm. Divide the PVA solvent into 8 equal parts. Each part of the PVA solvent is doped with two nanoparticles PVA/ (x) TiO₂ (15-x) ZnO for x=0, 1, 5, 7.5, 10, 14 and 15 wt% doping concentration. The doped PVA solvent is sonicated using ultrasonicator for 15 minutes. Then it is poured on to a petri dish and allowed to dry for 24 hours at 50°C using muffle furnace. The composite films are then peeled off from the Petri dish and kept in vacuum desiccators for further study.

3. RESULTS AND DISCUSSION

3.1 XRD Studies of nanocomposites

Bruker D₈ Advance X-ray diffractometer with Nickel filtered CuK α radiation of wavelength 1.5406Å and graphite monochromator is used to record the diffractograms in the range 2 θ = 5 to 120°. Figure 1 discloses the noticed XRD peaks of PVA/(x)TiO₂ (15-x) ZnO for x=0, 1, 5, 7.5, 10, 14 and 15 wt% doping concentration. Peaks at 2 θ = 25.44, 27.16, 41.20, 47.91, 54.43, 56.62, 63.4 and 69.35 represents TiO₂ nanoparticles whereas 2 θ =32.33, 35.15, 36.93, 48.49, 57.66, 64.23, 67.67, 69.35, 70.46, 74.29 represents the ZnO nanoparticles. This confirms the formation of PVA/(x)TiO₂ (15-x) ZnO nanocomposites. At 2 θ =19 to 20° a broad and widened semi-crystalline peaks is observed which corresponds to host PVA chain. The leading peaks of PVA shift towards the right side with the rise in dopant level up to x=14%. This suggests that crystallinity of the nanocomposite increases up to x=14% and more growth in dopant concentration exceeding x> 14%, the crystallinity decreases [9, 10]. The enhancement in crystalline nature is due the OH group of PVA binds with added nanoparticles establishing structural conformation.

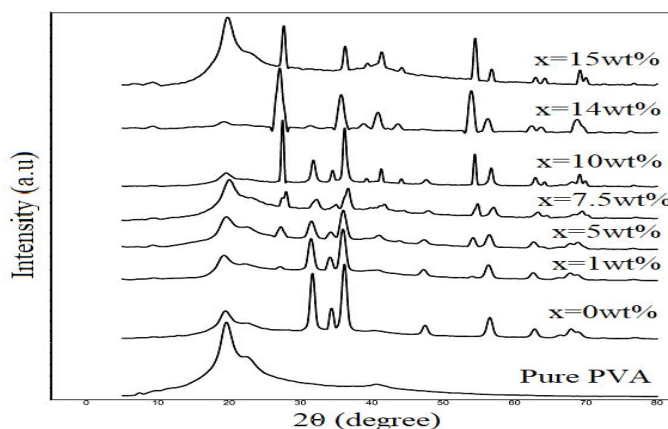


FIGURE 1: XRD spectra of PVA/(x)TiO₂ (15-x) ZnO for x=0, 1, 5, 7.5, 10, 14 and 15 wt%

3.2 UV-Visible Spectroscopy

The UV Visible spectra of all the films were recorded using JASCO V-630 UV-Visible spectrophotometer in the wavelength range of 100-900nm. The spectra of pure and doped PVA are shown in the Figure 2. PVA absorbs strongly in the wavelength range of 200-400nm and same is simulated in the figure as a shoulder like band at 279nm. Using Tauc's plots the optical energy band gaps are determined [11, 12]. Thus by plotting the product of absorption coefficient and photon energy ($\alpha h\nu$)² versus the photon energy (h ν) at room temperature shows a linear performance (Figure3). This linear behavior represents the direct allowed transitions that

happened between valence and conduction band. The observed lesser energy gap 2.45eV for 14 wt% doping concentration is due to local cross linking between interpenetrating polymer chain with added nanopopants. These added nanoparticles get coagulated with PVA which results in deceased molecular mobility to form a complex conformation. These factors increase the crystallinity thereby lessening in the energy gap [13, 8]. The energy gap changes from 4.66eV for pure PVA to 3.05eV, 2.88eV, 2.77eV, 2.71eV, 2.58eV, 2.45eV and 2.63eV respectively for x=0wt%, 1wt%, 5wt%, 7.5wt%, 10wt%, 14wt% and 15wt%.

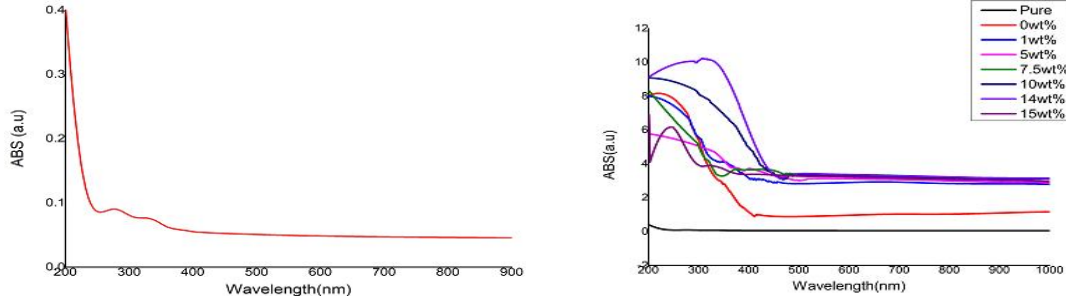


FIGURE 2: UV-Visible spectra of PVA and PVA/(x)TiO₂ (15-x) ZnO for x=0, 1, 5, 7.5, 10, 14 and 15 wt% doping

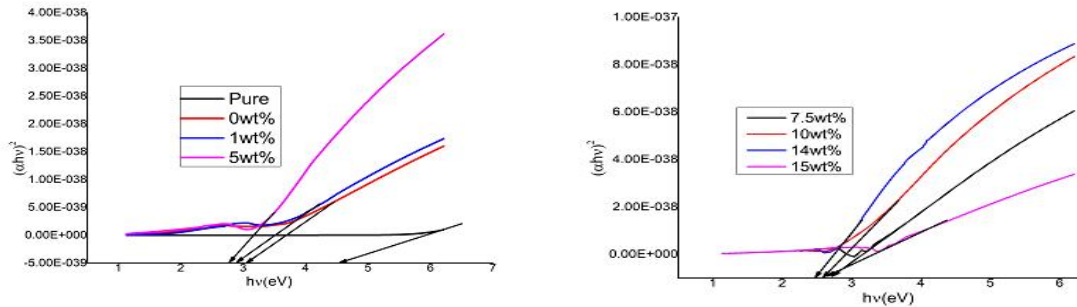


FIGURE 3: Optical energy gap of pure and PVA/(x) TiO₂ (15-x) ZnO for x=0, 1, 5, 7.5, 10, 14 and 15 wt% doping

3.3. Mechanical Studies of pure and doped PVA nanocomposites

Using universal testing machine (LLOYD LRX Plus-5 KN, UK) the tensile strength, stiffness, and Young's modulus of the various films were carried out. Figure 4 shows the Stress vs Strain graph of pure and doped PVA nanocomposites. The linear increase in the stress with rise in strain is observed in the elastic region. In the region of plastic deformation, there is no appreciable increase in stress with the enhancement in strain values. This happens due to the particulate nanoparticles added to the polymer matrix have large surface area [14]. Table 1 and figure 4 indicates that for x=14% the films exhibits high tensile strength and young's modulus. Also for x=14% doping high degree of crystallinity is observed from the XRD results. The degree of crystallinity and the morphology of the crystalline material deeply affect the mechanical behavior of the polymer.

TABLE 1: Mechanical properties of PVA/(x)TiO₂ (15-x) ZnO for x=0, 1, 5, 7.5, 10, 14 and 15 wt% doping

Dopant Concentration	Tensile Strength (MPa)	Stiffness (kN/m)	Young's Modulus (MPa)
Pure PVA	2.90	5.34	45.34
0 wt%	35.79	17.62	705.03
1 wt%	38.45	35.80	1193.33
5 wt%	41.60	32.72	1308.94
7.5 wt%	42.68	42.08	1402.75
10 wt%	44.10	30.14	1505.18
14 wt%	49.84	49.49	1649.75
15 wt%	37.19	33.91	847.84

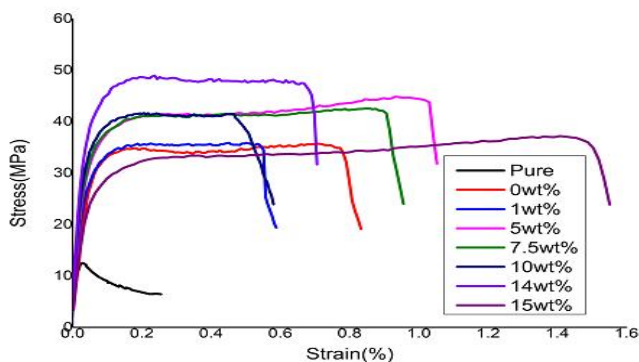


FIGURE 4: Stress- Strain curves of PVA/(x)TiO₂ (15-x) ZnO for x=0, 1, 5, 7.5, 10, 14 and 15 wt% doping

CONCLUSIONS

The XRD spectra confirm the formation of semi crystalline nature of the nanocomposites for x=14wt% optimized doping concentration. UV –Vis spectroscopy study shows drastic decrease in energy gap for x=14wt% doping concentration. The mechanical studies indicate for x=14wt% doping a high tensile strength of 49.84MPa and Young’s modulus of 1649.75MPa has been observed. Thus the doping of PVA with TiO₂ and ZnO nanoparticles improves the structural, optical and mechanical properties and finds application in material science.

REFERENCE

1. Falcoro, P. Application of metal and metal oxide nanoparticles. *Coordin. Chem. Rev.* **307**, 237–254 (2016)
2. Al-Ajmi, M. F., Hussain, A. & Ahmed, F. Novel synthesis of ZnO nanoparticles and their anticancer activity: Role of ZnO as a drug carrier. *Ceram. Int.* **42**, 4462–4469 (2016).
3. X. Bai, L. Li, H. Liu, L. Tan, T. Liu, and X. Meng, “Solvothermal synthesis of ZnO nanoparticles and anti-infection application in vivo,” *ACS Applied Materials and Interfaces*, vol. 7, no. 2, pp. 1308–1317, 2015.
4. U. Ozgür, Y. I. Alivov, C. Liu et al., “A comprehensive review of ZnO materials and devices,” *Journal of Applied Physics*, vol. 98, no. 4, Article ID 041301, 2005.
5. W. J. Jeong, S. K. Kim, and G. C. Park, “Preparation and characteristic of ZnO thin film with high and low resistivity for an application of solar cell,” *Thin Solid Films*, vol. 506-507, pp. 180–183, 2006.
6. M. Moritz and M. Geszke-Moritz, “The newest achievements in synthesis, immobilization and practical applications of antibacterial nanoparticles,” *Chemical Engineering Journal*, vol. 228, pp. 596–613, 2013.
7. Vasare, V., Zhang, Z., Avasare, D., Khan, I., Qurashi, A., 2015. Room-temperature synthesis of TiO₂ nanospheres and their solar driven photoelectrochemical hydrogen production. *Int. J. Energy Res.* **39**, 1714–1719. *Beilstein J. Nanotechnol.* **4**, 345–351.
8. Rithin Kumar N B, Vincent Crasta, B M Praveen & Mohan Kumar. Studies on Structural, Optical and Mechanical Properties of MWCNTs and ZnO nanoparticles doped PVA nanocomposites. *Nanotechnology Reviews*, **04**, 457-467 (2015).
9. Zidan, H. M. Structural properties of CrF₃, and MnCl₂-filled poly (vinyl alcohol) films. *J. Appl. Polym. Sci.* **88**, 1115–1120 (2003).
10. Rithinkumar N B, Vincent Crasta and B M Praveen, Dielectric and electric conductivity studies of PVA (Mowiol 10-98) doped with MWCNTs and WO₃ nanocomposites films, *Materials Research Express* **3** (5), 055012, 2016
11. N. F. Mott and E. A. Devis, *Electronic Process in Non-Crystalline Materials*, Oxford University Press, Oxford, UK, 2nd edition, 1979.
12. J. Tauc, *Optical properties of solids, Optical Properties of Solid*, F. Abeles, Ed., pp. 277, North-Holland, Amsterdam, The Netherlands, 1972.
13. M. S. Selim, R. Seoudi and A. A. Shabaka, Polymer based films embedded with high content of ZnSe nanoparticles, *Mater. Lett.*, Vol 59, 2005, pp. 2650–2654
14. Xia L, Xu Z, Sun L, Patrick M, Zhang CM, Zhang M (2013) *J Nanoparticle Res* **15**:1570